CHEMISTRY
A EUROPEAN JOURNAL

DOI: 10.1002/chem.201001982

A Second-Generation Photocage for Zn^{2+} Inspired by TPEN: Characterization and Insight into the Uncaging Quantum Yields of ZinCleav Chelators**

H. M. Dhammika Bandara, Timothy P. Walsh, and Shawn C. Burdette*[a]

Abstract: Photocages have been used to elucidate the biological functions of various small molecules and Ca^{2+}; however, there are very few photocages available for other metal ions. ZinCleav-2 (1-(4,5-dimethoxy-2-nitrophenyl)-*N*,*N*,*N*′,*N*′-tetrakis-pyridin-2-ylmethyl-ethane-1,2-diamine) is a second-generation photocage for Zn^{2+} that releases the metal ion after a light-induced bifurcation of the chelating ligand. The structure of ZinCleav-2 was inspired by TPEN (*N*,*N*,*N*′,*N*′-tetrakis(2-pyridylmethyl)ethylenediamine), which is routinely used to sequester metal ions in cells owing to its high binding affinity. Inclusion of a 2-nitrobenzyl chromophore leads to the formation of two more weakly binding di-(2-picolyl)amine (DPA) fragments upon photolysis of the TPEN backbone. The desired ligand was prepared using a modified procedure used to access ZinCleav-1 (1-(4,5-dimethoxy-2-nitrophenyl)-*N*,*N*′-dimethyl-*N*,*N*′-bis-pyridin-2-ylmethyl-ethane-1,2-diamine). ZinCleav-2 has a conditional dissociation constant (K_d) of ~0.9 fM as measured by competitive titration with a quinoline-based fluorescent sensor for Zn^{2+}. The K_d of the Zn^{2+} complex of the DPA photoproducts is ~158 nM; therefore, the ΔK_d for ZinCleav-2 photocage is ~10^8. A large ΔK_d is required to significantly perturb free metal ion concentrations in biological assays. The quantum yield of photolysis of apo ZinCleav-2 and the $[Zn(ZinCleav\text{-}2)]^{2+}$ complex are 4.7 and 2.3 %, respectively, as determined by HPLC analysis. Proof of concept Zn^{2+} release upon photolysis of $[Zn(ZinCleav\text{-}2)]^{2+}$ was demonstrated using the fluorescent sensor Zinpyr-1, and the speciation of Zn^{2+} complexes was simulated using computational methods. The influence of benzylic substituents on the quantum yield of uncaging is also analyzed with the aim of tuning the photochemical properties caged complexes for in vivo experiments.

Keywords: cage compounds · ligand effects · photolysis · photophysics · zinc

Introduction

Photoactive protecting groups were developed nearly 50 years ago to take advantage of light-induced removal strategies that are orthogonal to standard deprotection reactions.[1–3] Subsequently this methodology was expanded to engineer photocages that exploit the photolysis reaction to liberate biologically active species.[4–6] The first photocage consisted of an adenosine-5′-triphosphate (ATP) that was rendered biologically inert by linking an *o*-nitrobenzyl moiety to the terminal phosphate oxygen atom.[7] Irradiation of the photocage liberates ATP, which can then participate in normal physiological functions. This initial study demonstrated the feasibility of using photocaged compounds to study the biology of complicated, dynamic living systems. Photocages for a multitude of biomolecules including neurotransmitters,[8–10] inositols,[11,12] mRNA,[13] DNA,[14] peptides[15,16] and enzymes[17–19] have been reported subsequently. Understanding the function of these analytes in numerous processes has been facilitated through studies that can only be conducted with photocages. Although alternative photolabile groups, including ones that are amenable to 2-photon excitation, are the subject of significant research efforts, *o*-nitrobenzyl derived photocages remain the most commonly encountered protecting group for caging.[20,21]

Nitr-5 and Nitr-7, two caged metal complexes designed to release a metal cation upon irradiation, were reported by Tsien et al. nearly a decade after the introduction of caged-ATP.[22,23] The Nitr photocages consist of the Ca^{2+}-specific chelator BAPTA (1,2-bis(*o*-aminophenoxy)ethane-*N*,*N*,*N*′,*N*′-tetraacetic acid) covalently linked to a *o*-nitrobenzhydrol group attached to the aminophenoxy ring *para* to the amino group. Irradiation of the caged-Ca^{2+} complex converts the benzhydrol into a nitrosobenzophenone. The new resonance delocalization of the amino lone pair into the benzophenone carbonyl lowers the affinity of the BAPTA moiety for Ca^{2+}, which induces a release of the caged metal ion. This strategy has been exploited to gener-

[a] H. M. D. Bandara, T. P. Walsh, Prof. S. C. Burdette
Department of Chemistry, University of Connecticut
55 North Eagleville Road, Storrs, CT 06269-3060 (USA)
Fax: (+1) 860-486-2981
E-mail: shawn.burdette@uconn.edu

[**] TPEN = *N*,*N*,*N*′,*N*′-Tetrakis[2-pyridylmethyl]-ethylenediamine, ZinCleav-1 = 1-(4,5-dimethoxy-2-nitrophenyl)-*N*,*N*′-dimethyl-*N*,*N*′-bis-pyridin-2-ylmethylethane-1,2-diamine and ZinCleav-2 = 1-(4,5-dimethoxy-2-nitrophenyl)-*N*,*N*,*N*′,*N*′-tetrakispyridin-2-ylmethylethane-1,2-diamine.

Supporting information for this article is available on the WWW under http://dx.doi.org/10.1002/chem.201001982.

ate cages that release alkali earth metals,[24] Fe^{3+},[25] and Zn^{2+}.[26] Unlike photocages for organic molecules, where uncaging efficiency correlates primarily by the quantum yield of photolysis (Φ), the release of metal ions from caged complexes also depends on the difference in dissociation constant between the caged and uncaged chelator (ΔK_d = uncaged K_d/caged K_d). Although CrownCast and ZinCast compounds have greater ΔK_d (~400-fold) than Nitr cages (~40-fold), the quantum yields for all 2-nitrobenzhydrol derived caged complexes are small (<5%), so the increase in free metal ion concentration after flash photolysis remains modest.

To address the shortcomings of these caged complexes, Ellis-Davies and others developed an alternative uncaging strategy in which chelators with a high affinity for Ca^{2+} undergo bifurcation upon illumination.[27,28] The two resulting photoproduct fragments possess significantly lower affinity for Ca^{2+}, which releases the caged metal ion. Investigations of NP-EGTA and DM-nitrophen reveal that the reduction of chelate effects provides photocages possessing ΔK_d values of 10^4–10^5-fold (Scheme 1). Photolysis of the complexes occurs with quantum yields of between 18–23% (Table 1), which is significantly higher than those measured with *o*-nitrobenzhydrol derived cages. As a result, NP-EGTA and DM-nitrophen produce significantly larger increases in free Ca^{2+} concentration upon illumination; however, under intracellular conditions, DM-nitrophen exists as the Mg^{2+} complex.[29] As with Nitr cages, replacement of the Ca^{2+}-selective binding moiety with new ligands allows caging of other metals ions. A tetradentate chelator with amide and pyridyl ligands for caging Cu^{2+}, CuCage (Scheme 1) was recently reported.[30] The quantum yield of photolysis and ΔK_d for this caged-Cu^{2+} complex were 32% and 2×10^5-fold, respectively.

Table 1. Quantum yields of photolysis (Φ) of apo cages and caged metal complexes.[a]

Apo cage	Φ [%]	Caged complex	Φ [%]
ZinCleav-1[31],[b]	2.2	$[Zn(ZinCleav\text{-}1)]^{2+}$	1.7
ZinCleav-2[a]	4.7	$[Zn(ZinCleav\text{-}2)]^{2+}$	2.3
2[b]	10	$[Zn(\mathbf{2})]^{2+}$	8.7
3[b]	6.6	$[Ca(\mathbf{3})]^{2+}$	7.0
DM-Nitrophen[45],[c]	12	$[Ca(DM\text{-}Nitrophen)]^{2-}$	18
NP-EGTA[27],[d]	20	$[Ca(NP\text{-}EGTA)]^{2-}$	23
DMNPE-4[57],[e]	NA[g]	$[Ca(DMNPE\text{-}4)]^{2-}$	9.0
DMNPE-5[57],[e]	NA[g]	$[Ca(DMNPE\text{-}5)]^{2-}$	13
4[b]	17.2	NA[h]	NA
CuCage[30],[f]	73	[Cu(CuCage)]	32

[a] Quantum yields were determined by HPLC methodologies with the exception of the measurements of compounds **2**, **3** and **4** that were measured using UV/Vis spectroscopy. [b] Aqueous buffer (40 mM HEPES, 100 mM KCl, pH 7); 350 nm, 150 W Xe lamp; HPLC analysis. [c] Aqueous buffer (40 mM HEPES, 100 mM KCl, pH 7.2); ~300–400 nm, 1000 W filtered Hg acr lamp. [d] Aqueous buffer (10 mM HEPES, 130 mM KCl, pH 7.1); Ruby laser, 347 nm or ~300–400 nm, 1000 W filtered Hg acr lamp. [e] Aqueous buffer (40 mM HEPES, 100 mM KCl, pH 7.2); ~300–400 nm, 500 W filtered Hg acr lamp. [f] Phosphate buffer (NaH_2PO_4, pH 7.4); λ_{max} = 350 nm, 1200 W Rayonet-RPR-100 photoreactor. [g] No value for the apo-photocage is reported. [h] **4** does not interact strongly with Zn^{2+} under the experimental conditions.

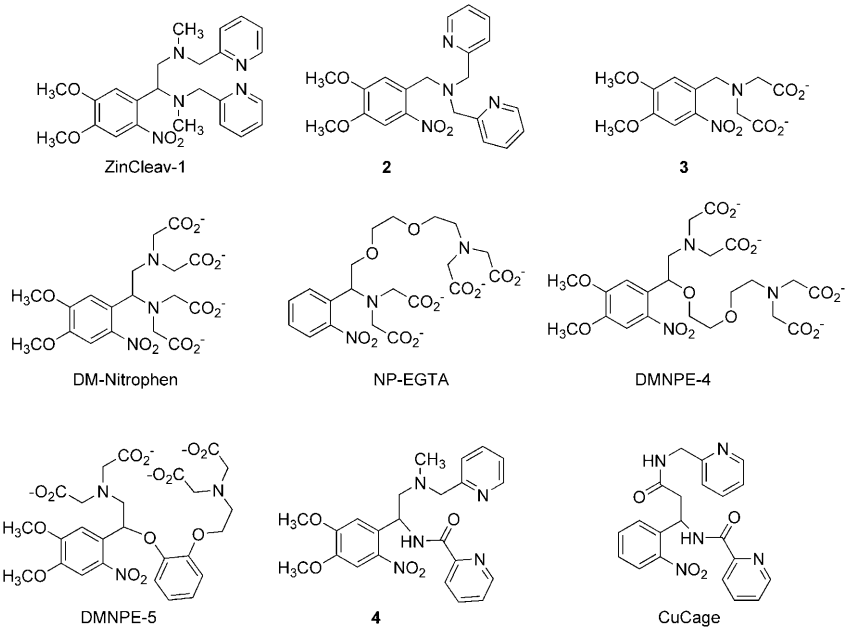

Scheme 1. Structures of metal ion photocages that fragment upon exposing the nitrobenzyl-based chelator to light.

Recently we demonstrated the release of Zn^{2+} upon photolysis of the photocaged complex $[Zn(ZinCleav\text{-}1)]^{2+}$.[31] ZinCleav-1 combines the tetradentate ligand EBAP (ethylene-bis-α,α′-(2-aminomethyl)-pyridine) with a 4,5-dimethoxy-2-nitrobenzyl chromophore (Scheme 1). The nomenclature ZinCleav refers both to the analyte of interest (*zinc*) and the mechanism of metal ion release (bond *cleavage*). Irradiation of $[Zn(ZinCleav\text{-}1)]^{2+}$ with 350 nm wavelength radiation generates two weakly Zn^{2+}-binding 2-(aminomethyl)pyridine fragments, which releases the bound metal ion. ZinCleav-1 possesses a high affinity for Zn^{2+} (K_d = 0.23 pM), whereas the affinities of the photofragments are significantly lower (K_d = ~40 mM), so the ΔK_d after uncaging is ~10^8. Despite binding Zn^{2+} tightly, Zn^{2+}-binding proteins like metallothionein ($K_d \approx 31$ fM)[32] have a higher affinity for the metal ion than the photocage. Since these metalloproteins potentially can extract Zn^{2+} from ZinCleav-1, a higher affinity caged complex would be desirable for conducting some in vitro experiments. In addition to the ΔK_d, the photolysis quantum yield of $[Zn(ZinCleav\text{-}1)]^{2+}$ of

0.55% measured by UV-visible spectroscopy is lower than the values reported for the structurally similar Cu^{2+}- and Ca^{2+}-caged complexes.

To address these issues, we sought to develop a second-generation ZinCleav complex with a higher affinity for Zn^{2+} and an improved quantum yield of photolysis. The hexadentate ligand TPEN (*N*,*N*,*N*′,*N*′-tetrakis(2-pyridylmethyl)-ethylenediamine) possesses a higher affinity for Zn^{2+} ($K_d = 0.4$ fM) than most metalloproteins.[33] Owing to its high affinity for Zn^{2+} and other transition metal ions, investigators routinely use TPEN to scavenge unwanted metal ions in cells,[34–36] to buffer intracellular free $[Zn^{2+}]$,[37] and as inspiration for the receptor in fluorescent sensors for biological imaging.[38–41] Although its high affinity makes TPEN a versatile chelator, prolonged exposure of live cells to excess TPEN induces apoptosis due to depletion of essential intracellular metal ions.[42] Access to a ZinCleav derivative utilizing a TPEN chelator would provide a caged complex that overcomes the intrinsic competition between proteins and ZinCleav-1 for Zn^{2+}, and keep the cage metalated until exposed to light. While the apo ligand would retain the toxicity of TPEN, the metallation of a TPEN-inspired photocage with Zn^{2+} would moderate the detrimental effects of introducing a high affinity chelator to cells.

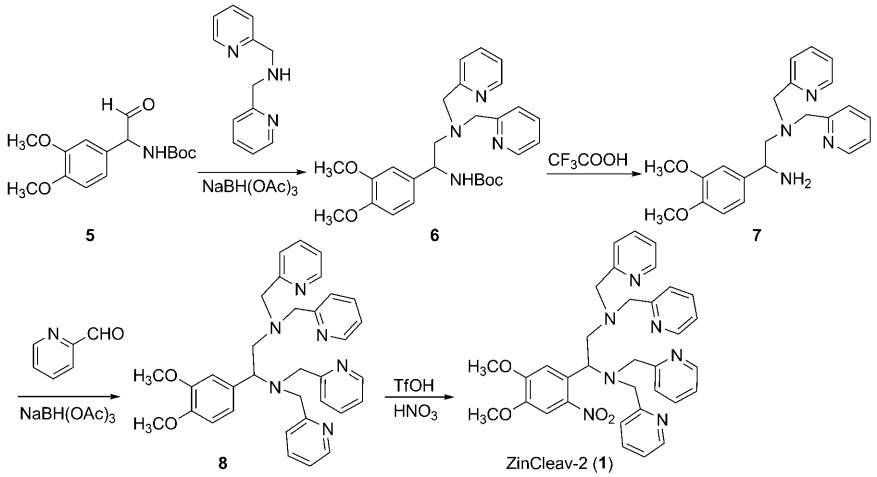

Scheme 3. Synthesis of ZinCleav-2.

Results and Discussion

We designed the TPEN-inspired photocage ZinCleav-2 based on the ZinCleav-1 scaffold. Similar to ZinCleav-1, photolysis of ZinCleav-2 would generate two di-(2-picolyl)-amine fragments (DPA, Scheme 2). Since DPA binds Zn^{2+} more tightly than the photoproducts of ZinCleav-1, the final resting free Zn^{2+} would be buffered at lower concentrations after photolysis of ZinCleav-2. The desired caged-Zn^{2+} complex, $[Zn(ZinCleav\text{-}2)]^{2+}$ was accessed by modifying the route used to prepare ZinCleav-1 (Scheme 3). Starting with 3,4-dimethoxybenzaldehyde, aldehyde **5** was synthesized as described previously.[31] Reductive amination of **5** in the presence of DPA provided the protected amine **6**. Deprotection of **6** followed by reductive amination with two equivalents of 2-pyridinecarboxaldehyde yielded the modified TPEN ligand **8** with an overall yield of 28.5% over three steps. Approximately 1 g of the TPEN ligand (unnitrated ZinCleav-2) can be generated in three steps starting with 3 g of **5**. Attempts to recrystallize **8** as the hydrochloric acid salt were unsuccessful due to decomposition of the ligand. Nitration of **8** was carried out at −40 °C with triflic acid (CF_3SO_3H) and fuming nitric acid. The yield of the nitration step was low (14%) compared to that of ZinCleav-1 (39%) possibly due to the apparent acid sensitivity of **8**. Although the yield of the nitration reaction is low, the synthesis of ZinCleav-2 further demonstrates the versatility of our new methods for preparing nitrobenzyl derived metal ion chelators.

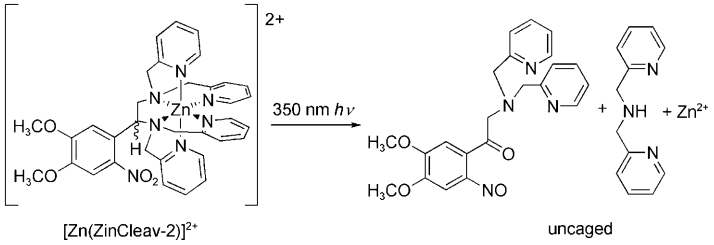

Scheme 2. Uncaging action of $[Zn(ZinCleav\text{-}2)]^{2+}$.

The apparent dissociation constant (K_d) of $[Zn(ZinCleav\text{-}1)]^{2+}$ was determined by competitive titration with 4-(2-pyridyl-2-azo)resorcinol (PAR); however, this technique was not sufficiently sensitive to measure the K_d of the $[Zn(ZinCleav\text{-}2)]^{2+}$ complex. Potentiometric titrations to determine the Zn^{2+} binding constants and pK_a values of ZinCleav-2 also were unsuccessful due to the acid sensitivity of the ligand and its limited solubility in water at mM concentrations. Alternatively we envisioned using a different chelator with a fluorescent reporting group as a ligand for competitive titrations. A quinoline-based Zn^{2+} sensor with a $K_d = 0.45$ fM was recently reported.[43] This sensor forms a 1:1 complex with Zn^{2+} with a concomitant increase in fluorescence emission at 438 nm. The sensor was synthesized as described, and used in competitive titrations under simulated physiological conditions (25 mM HEPES, 100 mM $NaClO_4$, pH 7.4, Scheme 4). The data were corrected for ligand protonation using pK_a values reported for TPEN. Analysis in triplicate provided an apparent K_d of 0.9 ± 0.1 fM for ZinCleav-2 at pH 7.4, which is in agreement with the parent

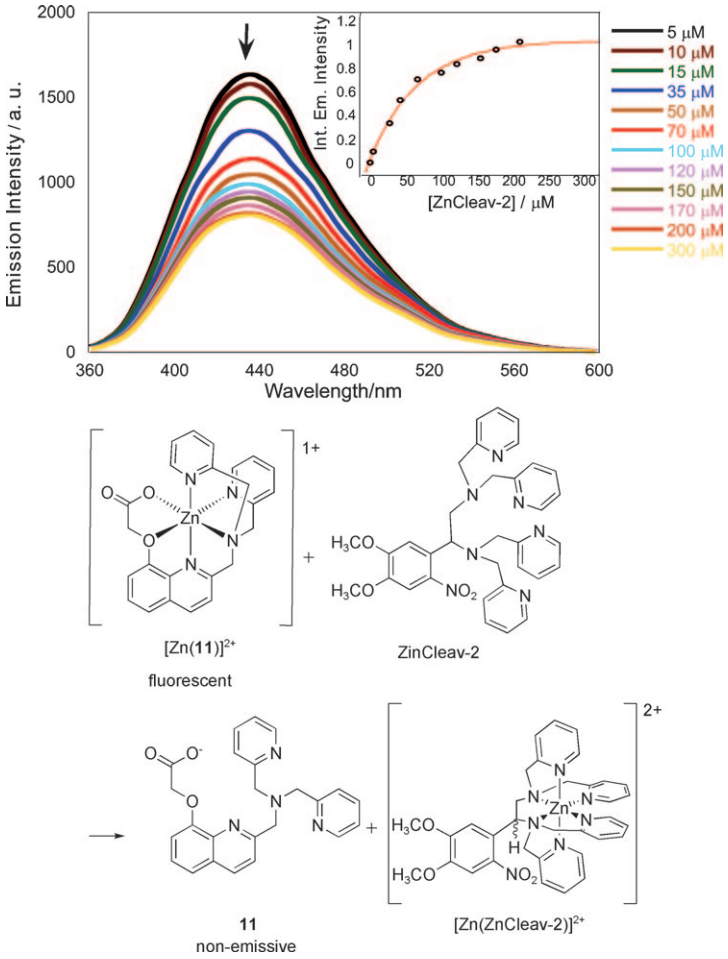

Scheme 4. Competitive titration between ZinCleav-2 and the Zn^{2+} sensor 11 in the presence of Zn^{2+}. A 10 μM solution of the Zn^{2+} sensor (25 mM HEPES, 100 mM $NaClO_4$, pH 7.4) and 5 μM $Zn(ClO_4)_2$ was titrated against a solution of ZinCleav-2 and emission intensity was measured after each addition. The K_d was calculated by monitoring the decrease in emission intensity.

TPEN ligand under the same conditions (K_d = 0.2 fM). The K_d of the Zn^{2+} complex of DPA is 158 nM;[44] therefore, ZinCleav-2 has a ΔK_d of ~10^8. Introduction of excess Cu^{2+} to $[Zn(ZinCleav\text{-}2)]^{2+}$ induces a ligand exchange reaction as predicted by the Irving–Williams series; however the low concentration of free Cu^{2+} in cells would prevent Zn^{2+} displacement. Ca^{2+} does not bind ZinCleav-2 or displace Zn^{2+} from $[Zn(ZinCleav\text{-}2)]^{2+}$ under physiological conditions.

To determine the quantum yield of ZinCleav-2, changes in the UV/Vis spectrum were measured during the course of the photolysis reaction, and the number of photons was determined using actinometry. Using optical methods, the quantum yield of ZinCleav-2 and $[Zn(ZinCleav\text{-}2)]^{2+}$ were calculated to be 5.0 and 0.59%, respectively. Like the measurements with ZinCleav-1, the apo-ligand uncaged with a quantum yield of ~5%, which decreased by nearly an order of magnitude in the presence of Zn^{2+}. Since the quantum yields deviated significantly from the values reported for structurally similar caged complexes, the efficiency of the photolysis reaction was interrogated further.

Repeating the quantum yield measurements using HPLC to assess the progress of the photolysis provided slightly different results for the efficiency of the uncaging. While the quantum yields of photolysis measured for apo-ZinCleav-2 by UV/Vis (5.0%) and HPLC (4.7%) are within experimental error, the uncaging of $[Zn(ZinCleav\text{-}2)]^{2+}$ appears to be more efficient when using HPLC to monitor the disappearance of the starting material. Further analysis of the HPLC traces suggest that the photoproducts of ZinCleav-2 undergo secondary reactions in the presence of the uncaged metal ions, which would lead to deviation in the quantum yields measured spectrophotometrically. Similar observations have been made with Ca^{2+} photocages.[45] In addition to the measurements with ZinCleav-2, the quantum yields of photolysis for ZinCleav-1 and $[Zn(ZinCleav\text{-}2)]^{2+}$ were reassessed by HPLC. The results with apo-ZinCleav-1 are consistent with the values determined by UV/Vis spectroscopy; however, $[Zn(ZinCleav\text{-}1)]^{2+}$ uncages more efficiently than previously determined (Table 1).

Release of Zn^{2+} upon photolysis of $[Zn(ZinCleav\text{-}2)]^{2+}$ was demonstrated by uncaging the complex in the presence of the fluorescent sensor Zinpyr-1.[46] Zinpyr-1 has a K_d of 0.04 pM for Zn^{2+},[47] and when Zn^{2+} (5 μM) is added to a solution of 30 μM Zinpyr-1 (40 mM HEPES, 100 mM KCl, pH 7.4) an enhancement in emission is observed. The fluorescence signal returns to near its initial intensity upon the addition of 40 μM ZinCleav-2. Irradiation of the solution with a 900 W source causes photolysis of $[Zn(ZinCleav\text{-}2)]^{2+}$ and release of Zn^{2+} resulting in complete recovery of the fluorescence signal (Scheme 5). The fluorescence assay is consistent with the fragmentation of the ZinCleav-2 ligand, and Zinpyr-1 scavenging the Zn^{2+} from the more weakly binding DPA photoproducts.

Caged complexes derived from *o*-nitrobenzyl groups have widely varying quantum yields of photolysis. Caged complexes with high quantum yields are desirable; however, there are no clear rules for predicting the uncaging efficiency of nitrobenzyl derivatives. The photoreaction of *o*-nitrobenzyl groups has been the subject of numerous mechanistic studies. Uncaging requires the light-induced generation of an *aci*-nitro intermediate that undergoes rearrangement and fragmentation to release the analyte (Scheme 6, red).[48,49] We hypothesized that the low uncaging quantum yields of the ZinCleav complexes might be explained by the generation of an intermediate with decreased *aci*-nitro character. To test this hypothesis, we synthesized a series of *o*-nitrobenzyl derivatives and compared the quantum yields to the ZinCleav complexes and the analogous photocages for other metal ions. The most likely interference with the formation of the *aci*-nitro intermediate would be a resonance interaction with a heteroatom attached to the benzylic carbon atom (Scheme 6, blue). In such a mechanism, *o*-nitrobenzyl cages with strong electron donors like nitrogen atoms at the benzylic position would be expected to have

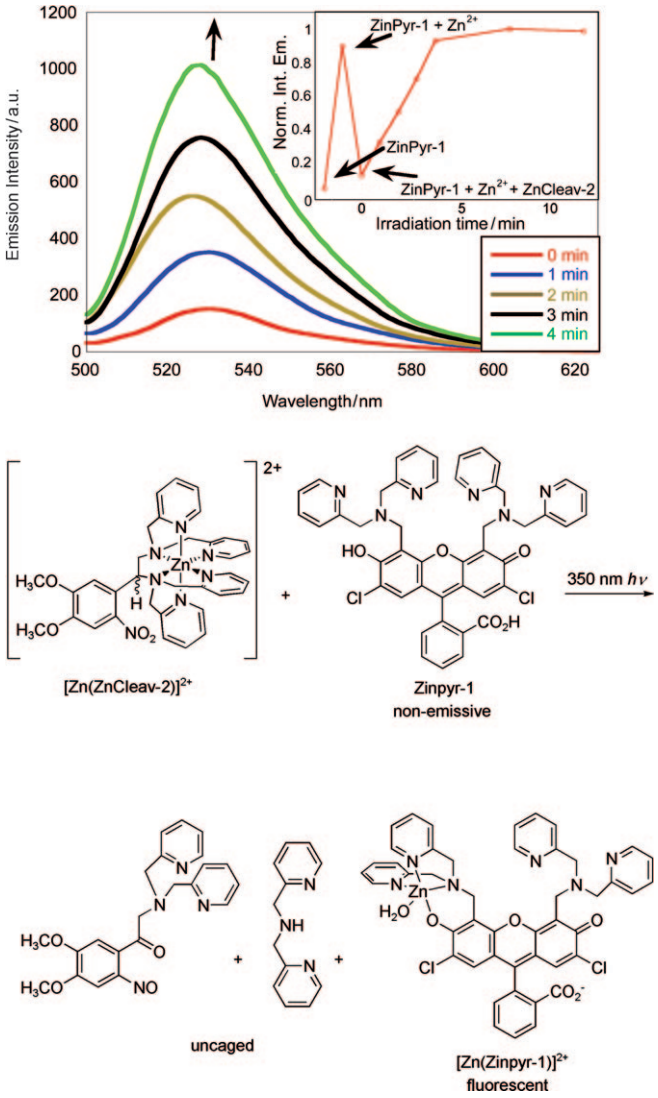

Scheme 5. Fluorescence response of Zinpyr-1 upon uncaging of ZinCleav-2 (top). The emission intensity of a solution of 5.0 μM Zinpyr-1 (40 mM HEPES, 100 mM KCl, pH 7.4) was recorded before and after the addition of 30 μM $ZnCl_2$. The emission was integrated between 500–600 nm and normalized to the maximum response (inset). Subsequent addition of 40 μM ZinCleav-2 quenched the emission of the Zinpyr-1 complex, which has a K_d of 0.10 nM for Zn^{2+}. Irradiation of the solution in a Rayonet RPR-100 photoreactor resulted in a complete photolysis of ZinCleav-2 within 4 min. This behavior is consistent with Zinpyr-1 acquiring Zn^{2+} from the photolyzed ZinCleav-2 (bottom).

the lowest quantum yields of photolysis. Coordination of the nitrogen atoms to a metal ion should mitigate the resonance interaction and increase the quantum yield.

Initially model photocages **2** and **3** were prepared to delineate the effect of ancillary ligands on the quantum yield of cages containing benzylic amine groups (Scheme 1 and Table 1). The modest difference in quantum yield suggests that carboxylate and pyridine groups do not influence the photochemistry. The presence of Ca^{2+} enhances the photolysis efficiency of **3**, while Zn^{2+} slightly decreases the quantum yield of **2**; however, quantum yields of both the apo ligands and the complexes are the same within experimental error.

Quantum yields of the Ellis–Davies photocages containing benzylic nitrogen ligands increase in the presence of Ca^{2+}. This behavior is consistent with the proposed mechanism since a lone pair involved in a bonding interaction would be less available to engage in resonance interactions with the *aci*-nitro intermediate. Unexpectedly, the quantum yields of ZinCleav-1 and ZinCleav-2 decrease in the presence of Zn^{2+}. Since ZinCleav compounds do not bind Ca^{2+}, additional quantum yield measurements with the Zn^{2+} complexes of DM-Nitrophen and NP-EGTA could provide important insight into reasons for the deviation from expected behavior. Additional support of the *aci*-nitro deactivation mechanism can be garnered from the quantum yield measured for *o*-nitrobenzyl cages bearing benzylic amides. Amide nitrogen atoms are weak electron donors owing to the resonance delocalization of the nitrogen lone pair of electrons onto the carbonyl oxygen. The quantum yields of apo-CuCage[30] and compound **4** provide supportive evidence that diminished resonance with the *aci*-nitro intermediate increases the quantum yield, and is consistent with cages for organic amides.[50]

Although the nature of the leaving group and other factors probably influence the uncaging efficiency, additional time-resolved spectroscopic experiments will be required to fully delineate the contribution of each variable. The effects of variances in methodologies used to determine quantum yields and different light sources also cannot be quantified in this initial analysis that relies on previously published reports. Preliminary observations with ZinCleav complexes as well as compounds **2**, **3** and **4** suggest a clean conversion to the expected products when using monochromatic light, but a different slate of products is formed when using a broad spectrum light source. Future investigations will focus on explaining this phenomenon as well as designing photocages that account for the photochemistry of the *aci*-nitro intermediate.

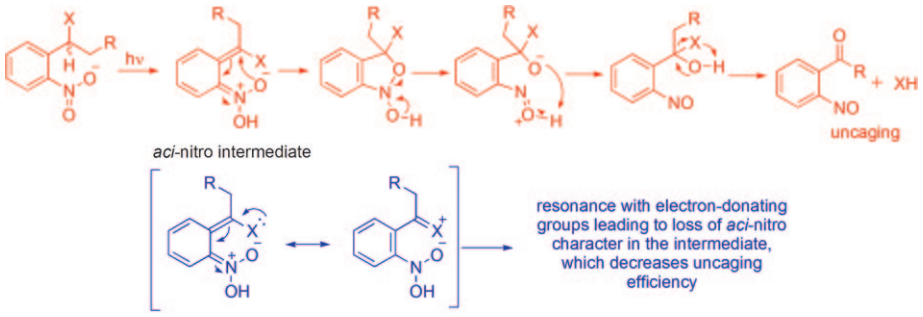

Scheme 6. Uncaging mechanism in ZinCleav-2 and related chelators (top), and proposed pathway for the deactivation of the *aci*-nitro intermediate by electron donation from benzylic heteroatoms (bottom).

Zinc is essential for the proper function of cells, but since it is cytotoxic at high concentrations, intracellular Zn^{2+} must be tightly regulated. Metalloproteins and other chelators

tightly bind and sequester Zn^{2+}; however, eukaryotic cells may contain a small pool of weakly bound or chelatable zinc. Measurements of free Zn^{2+} for different cell lines put the amount at low levels between 5 pM and ~2 nM.[51–54] No detectable free Zn^{2+} exists in prokaryotic cells, however, values as low as 0.5 fM have been estimated.[55] The total concentration of zinc binding chelators in cells and their average affinity for Zn^{2+} are also known for different cell types. With this information it is possible to calculate the exogenous [ZinCleav]/[Zn^{2+}] ratio required to maintain the intracellular free Zn^{2+} at physiologically normal levels. We chose six hypothetical scenarios to simulate buffering the resting free Zn^{2+} with ZinCleav caged complexes. Concentration of 1 fM, 10, 100, 500 and 790 pM were selected based on studies of estimated free Zn^{2+} concentrations in different cell lines, and the absolute Zn^{2+} and zinc-binding chelator concentrations were assumed to be 250 and 275 μM, respectively. These values closely match the typical concentrations in cells.[53]

Fluctuations in the intracellular free Zn^{2+} concentration following photolysis of the caged complex can be simulated with HySS, a computer program for modeling speciation in solution.[56] Of the two ZinCleav caged-zinc complexes, only the TPEN-based photocage ZinCleav-2 has the capacity to maintain free Zn^{2+} at low fM concentrations under resting conditions and still generate a significant increase in free Zn^{2+} after photolysis (Table 2). A [ZinCleav-2]/[Zn^{2+}] ratio of 1:1 maintains Zn^{2+} at pM concentrations, and a slight excess of apo-chelator can buffer Zn^{2+} in the fM regime. In contrast, a significant excess ZinCleav-1 is necessary to prevent perturbing Zn^{2+} homeostasis when the resting concentration is between 1–10 pM (Table 3). In addition to requiring excess apo-photocage which may not have the same biodistribution as the caged complex in a dynamic cellular environment, the increase in free Zn^{2+} following photolysis of [Zn(ZinCleav-1)]$^{2+}$ is smaller because the excess chelator buffers the released Zn^{2+}. At initial Zn^{2+} concentrations higher than 100 pM, the increase in Zn^{2+} following photolysis of [Zn(ZinCleav-2)]$^{2+}$ is lower than those simulated with ZinCleav-1. The higher Zn^{2+} affinity of the tridentate DPA photoproducts sequester uncaged Zn^{2+} more efficiently than the bidentate aminomethylpyridine photoproducts formed after ZinCleav-1 photolysis. Strategies for manipulating ZinCleav-2 in cells and applying these photocages to problems in Zn^{2+} biology are ongoing.

Table 2. Free [Zn^{2+}] buffering using ZinCleav-2.[a]

Resting [Zn^{2+}]	Added ZinCleav-2	Added Zn^{2+}	[Zn^{2+}] with 10% uncaging	[Zn^{2+}] with 25% uncaging	[Zn^{2+}] with 50% uncaging
1 fM	50 μM	40 μM	1.2 fM	1.6 fM	3.1 fM
1 pM	50 μM	50 μM	1.2 pM	2.1 pM	29.5 pM
10 pM	50 μM	50 μM	12.7 pM	21.0 pM	935 pM
100 pM	50 μM	50 μM	127 pM	209 pM	2.9 nM
500 pM	50 μM	50 μM	637 pM	1.04 nM	6.7 nM
790 pM	50 μM	50 μM	1.0 nM	1.60 nM	8.5 nM

[a] Calculations are based on a total cellular [Zn^{2+}] of 250 μM and a cellular chelator concentration of 275 μM. Speciation was simulated and concentrations were calculated with HySS. ZinCleav-1 photoproducts were assumed to have logβ = 4.4.

Conclusion

The key intermediate aldehyde **5** enables a variety of zinc cages with different binding as well as photochemical properties to be accessed. The affinity of ZinCleav-2 for Zn^{2+} was increased significantly over ZinCleav-1 by increasing the number of chelating pyridyl groups to provide a TPEN-like chelator. Computational simulations demonstrate that ZinCleav-2 can be used to buffer Zn^{2+} at intracellular concentrations ranging from fM to sub-nM, which are typical levels found in cells. The high fM affinity of ZinCleav-2 prevents perturbation of Zn^{2+} homeostasis prior to uncaging, which is more difficult to accomplish with the first generation photocage ZinCleav-1 that has a pM K_d for Zn^{2+}. Although we discovered that HPLC methodologies provide more accurate measurements of the quantum yields of [Zn(ZinCleav)]$^{2+}$ complexes and that the quantum yields of ZinCleav caged complexes are higher than originally believed, ZinCleav cages have lower quantum yields of photolysis when compared with the typically low uncaging efficiency of all *o*-nitrobenzyl compounds. The low quantum yields are attributed to the formation of an intermediate that closely resembles the *aci*-nitro one that is the key precursor in the uncaging mechanism by resonance interactions from benzylic heteroatoms. The quantum yield of photolysis of the caged complex can be improved by installing an amide substituent or other functional group at the benzylic position that does not donate electrons by resonance; however, these changes also

Table 3. Free [Zn^{2+}] buffering using ZinCleav-1.[a]

Resting [Zn^{2+}]	Added [ZinCleav-1]	Added [Zn^{2+}]	[Zn^{2+}] with 10% uncaging	[Zn^{2+}] with 25% uncaging	[Zn^{2+}] with 50% uncaging
1 fM	50 μM	13 μM	1.0 fM	1.0 fM	1.1 fM
1 pM	50 μM	40 μM	1.1 pM	1.5 pM	3.3 pM
10 pM	50 μM	49 μM	12.7 pM	20.0 pM	280 pM
100 pM	50 μM	50 μM	128 pM	211 pM	34.9 nM
500 pM	50 μM	50 μM	639 pM	1.05 nM	78 nM
790 pM	50 μM	50 μM	1.0 nM	1.67 nM	98 nM

[a] Calculations are based on a total cellular [Zn^{2+}] of 250 μM and a cellular chelator concentration of 275 μM. Speciation was simulated and concentrations were calculated with HySS. ZinCleav-2 photoproducts were assumed to have logβ 6.8.

compromise the metal binding properties of the ligand. In order to design caged complexes that uncage efficiently, additional investigations into the mechanism of uncaging will need to be conducted, and new strategies for ligand construction will need to be devised. Other properties of the cages will also need to be optimized to ensure that the photocages are appropriate for the desired biological applications. Synthesis and characterization of improved ZinCleav derivatives are in progress.

Experimental Section

General synthetic procedures: All reagents were purchased from Acros at the highest commercial quality and used without further purification unless otherwise stated. [1-(3,4-dimethoxyphenyl)-2-oxo-ethyl]-carbamic acid *tert*-butyl ester (**5**),[31] di-(2-picolyl)amine (DPA),[44] 9-(*o*-carboxyphenyl)-2,7-dichloro-4,5-bis[bis(2-pyridylmethyl)-aminomethyl]-6-hydroxy-3-xanthanone (Zinpyr-1, **10**),[46] and {2-[(bis-pyridin-2-ylmethyl-amino)-methyl]-quinolin-8-yloxy}-acetic acid sodium salt (**11**)[43] were synthesized according to literature procedures. Dichloromethane (CH_2Cl_2) and tetrahydrofuran (THF) were sparged with argon and dried by passage through a Seca Solvent Purification System. All chromatography and TLC were performed on silica (230–400 mesh) from Silicycle unless otherwise specified. TLCs were developed with mixtures of CH_2Cl_2/CH_3OH or CH_2Cl_2/CH_3OH/NH_4OH unless otherwise specified and were visualized with 254 and 365 nm light. ^1H and ^{13}C NMR spectra were recorded using a Bruker 400 MHz NMR instrument and chemical shifts are reported in ppm on the δ scale relative to tetramethylsilane. IR spectra were recorded on a Nicolet 205 FT-IR instrument and the samples were prepared as KBr pellets or thin films on KBr plates. High resolution mass spectra were recorded at the University of Connecticut mass spectrometry facility using a micromass Q-Tof-2TM mass spectrometer operating in positive ion mode.

(4,5-Dimethoxy-2-nitro-benzyl)-pyridin-2-ylmethyl-pyridin-3-ylmethyl-amine (2): 6-nitroveratraldehyde (113 mg, 0.54 mmol), DPA (107 mg, 0.54 mmol) and $NaBH(OAc)_3$ (172 mg, 0.81 mmol) were combined in 1,2-dichloroethane (10 mL). The resulting solution was stirred at 23 °C for 18 h. Water (20 mL) was added and the product was extracted into CH_2Cl_2 (3×10 mL). The organic layers were combined, dried over $MgSO_4$, and the solvent was removed. Flash chromatography on silica (47:3 CH_2Cl_2/CH_3OH) yielded **6** as a yellow oil (152 mg, 72.7 %). TLC R_f=0.76 (silica, 93:7:1 CH_2Cl_2/CH_3OH/NH_4OH); ^1H NMR (400 MHz, $CDCl_3$): δ = 8.47 (d, J=4.3 Hz, 2H, ArH), 7.57 (dd, J=11.5, 3.6 Hz, 3H, ArH), 7.47 (s, 1H, ArH), 7.38 (d, J=7.8 Hz, 2H, ArH), 7.09–7.06 (t, J= 6.7 Hz, 2H, ArH), 4.09 (s, 2H, CH_2), 3.95 (s, 4H, CH_2), 3.84 (s, 3H, CH_3), 3.82 ppm (s, 3H, CH_3); ^{13}C NMR (100 MHz, $CDCl_3$): δ = 159.1, 153.1, 149.3, 147.5, 141.5, 136.5, 130.6, 123.2, 122.3, 112.7, 108.3, 60.6, 56.7, 56.5, 56 ppm; IR (thin film): $\tilde{\nu}$ = 3063.5, 3008.5, 2935.2, 2832.9, 1613.9, 1588.3, 1576.2, 1524.5, 1463.8, 1433.5, 1325.3, 1269.2, 1213.8, 1186.9, 1149.4, 1061.3, 1033.6, 993.2, 873.4, 794.5, 762.7, 730.3 cm^{-1}; HRMS (ESI+): m/z: calcd for: 394.1641; found: 394.1655 [M+H^+].

[(4,5-Dimethoxy-2-nitro-benzyl)-ethoxycarbonylmethyl-amino]-acetic acid ethyl ester (9): 6-Nitroveratraldehyde (602 mg, 2.85 mmol), iminodiacetic acid diethyl ester (500 μL, 2.85 mmol) and $NaBH(OAc)_3$ (906 mg, 4.27 mmol) were combined in 1,2-dichloroethane (50 mL). The resulting solution was stirred at 23 °C for 18 h. Water (20 mL) was added and the product was extracted into CH_2Cl_2 (3×10 mL). The organic layers were combined, dried over $MgSO_4$, and the solvent was removed. Flash chromatography on silica (24:1 CH_2Cl_2/CH_3OH) yielded **9** as a yellow solid (450 mg, 44.2 %). TLC R_f=0.45 (1:1 CH_2Cl_2/hexanes); m.p. 62–64 °C; ^1H NMR (400 MHz, $CDCl_3$): δ = 7.67 (s, 1H, ArH), 7.61 (s, 1H, ArH), 4.30 (s, 2H, CH_2), 4.18 (q, J=7.1 Hz, 4H, CH_2), 4.01 (s, 3H, CH_3), 3.95 (s, 3H, CH_3), 3.58 (s, 4H, CH_2), 1.28 ppm (t, J=7.1 Hz, 6H, CH_3); ^{13}C NMR (100 MHz, D_2O): δ = 179.9, 153.2, 146.9, 141.2, 131.2, 113.2, 108.7, 58.6, 56.6, 56.3, 54.9 ppm; IR (thin film): $\tilde{\nu}$ = 3066.6, 2978.4, 2919.1, 1729.4, 1740.3, 1576.6, 1514.9, 1470.5, 1436.8, 1369.4, 1324.9, 1196.4, 1161.0, 1060.4, 1022.1, 982.9, 906.7, 847.7, 793.4, 756.8, 736.9 cm^{-1}; HRMS (ESI+): m/z: calcd for: 384.1533; found: 384.1547 [M+H^+].

[Carboxymethyl-(4,5-dimethoxy-2-nitro-benzyl)-amino]-acetic acid (3): Diester **9** (49 mg, 0.13 mmol) was dissolved in 1,4-dioxane (1.4 mL) and treated with 1 M KOH (630 μL). The resulting solution was stirred at 23 °C for 18 h. The pH of the solution was adjusted to 2 with concentrated HCl and the solution was left at −10 °C for 18 h. The desired product precipitated as yellow crystals (7.0 mg, 15.5 %). M.p. 210–212 °C; ^1H NMR (400 MHz, D_2O): δ = 7.55 (s, 1H, ArH), 7.43 (s, 1H, ArH), 3.99 (s, 2H, CH_2), 3.99 (s, 3H, CH_3), 3.89 (s, 3H, CH_3), 3.10 ppm (s, 4H, CH_2); ^{13}C NMR (100 MHz, D_2O): δ = 179.9, 153.2, 146.9, 141.2, 131.2, 113.2, 108.7, 58.6, 56.6, 56.3, 54.9 ppm; IR (thin film): $\tilde{\nu}$ = 3322.4, 3032.1, 2989.4, 2890.3, 1727.3, 1577.0, 1502.4, 1480.8, 1370.5, 1279.5, 1230.3, 1187.7, 1059.2, 981.3, 902.1, 796.4, 674.7 cm^{-1}; HRMS (ESI+): m/z: calcd for: 328.0907; found: 328.0913 [M+H^+].

Pyridine-2-carboxylic acid [(4,5-dimethoxy-2-nitro-phenyl)-(methyl-pyridin-2-ylmethyl-amino)-methyl]-amide (4): Picolinic acid (122 mg, 0.99 mmol) and *N*-methylmorpholine (0.11 mL, 0.99 mmol) were combined in CH_2Cl_2 (3.5 mL) and cooled to 0 °C. A solution of benzotriazolyloxytris(dimethyl-amino)phosphoniumhexafluorophosphate (BOP, 438 mg, 0.99 mmol) in CH_2Cl_2 (2.5 mL) was added and the resulting mixture was stirred at 23 °C for 18 h. A solution of 1-(3,4-dimethoxy-phenyl)-*N*′-methyl-*N*′-pyridin-2-ylmethyl-ethane-1,2-diamine (300 mg, 0.99 mmol) in DMF (17 mL) was added and the resulting solution was stirred at 23 °C for18 h. The solvent was removed, saturated aqueous NaCl (15 mL) was added and the product was extracted into CH_2Cl_2 (3×10 mL). The organic layers were combined, dried over $MgSO_4$, and the solvent was removed. The crude product (264 mg, 0.48 mmol) and $Cu(NO_3)_2$·$3H_2O$ were combined in Ac_2O (1 mL) and stirred at 0 °C for 8 h. Water (5 mL) was added and the product was extracted into CH_2Cl_2 (3×10 mL). The organic layers were combined, washed with 1.0 M solution of EDTA (pH 11), dried over $MgSO_4$ and the solvent was removed. Flash chromatography on silica (91:8:1 CH_2Cl_2/CH_3OH/NH_4OH) yielded **4** as a yellow oil (34.1 mg, 7.6 %). ^1H NMR (400 MHz, $CDCl_3$): δ = 8.73 (s, 1H, NH), 8.54–8.50 (m, 2H, ArH), 7.66 (dd, J=1.0, 6.7 Hz, 1H, ArH), 7.63–7.7.59 (m, 1H, ArH), 7.45 (d, J=7.7 Hz, 1H, ArH), 7.28–7.24 (m, 2H, ArH), 7.19–7.15 (m, 3H, ArH), 4.65 (dd, J=12.3, 5.1 Hz, 1H, CH), 3.86 (s, 3H, CH_3), 3.83 (s, 3H, CH_3), 3.72 (d, J=4.0 Hz, 1H, CH_2), 3.61 (d, J=4.0 Hz, 1H, CH_2), 2.70 (dd, J=12.3, 16.1 Hz, 1H, CH_2). 2.61 (dd, J=5.1, 12.3 Hz, 1H, CH_2), 2.1 ppm (s, 3H, CH_3); ^{13}C NMR (100 MHz, $CDCl_3$): δ = 172.3, 159.1, 157.5, 149.5, 149.2, 149.1, 136.9, 136.7, 129.1, 123.1, 122.4, 122.3, 122.2, 122.0, 112.2, 111.2, 61.3, 57.0, 56.1, 44.7, 40.6 ppm; IR (thin film): $\tilde{\nu}$ = 3012.1, 2924.5, 2853.4, 1652.9, 1521.4, 1506.3, 1457.1, 1436.5, 1374.4, 1339.0, 1277.6, 1220.2, 1174.9, 1094.6, 1056.4, 946.7, 842.9, 746.7 cm^{-1}; HRMS (ESI+): m/z: calcd for: 451.1856; found: 451.1861 [M+H^+].

[2-(Bispyridin-2-ylmethylamino)-1-(3,4-dimethoxyphenyl)ethyl]-carbamic acid *tert*-butyl ester (6): Aldehyde **5** (2.45 g, 8.30 mmol), DPA (1.65 g, 8.30 mmol), $NaBH(OAc)_3$ (2.78 g, 13.3 mmol) and AcOH (0.50 mL, 8.70 mmol) were combined in CH_2Cl_2 (50 mL). The reaction was stirred at 23 °C for 24 h. Saturated Na_2CO_3 (30 mL) was added and the product was extracted into CH_2Cl_2 (3×60 mL). The combined organic extracts were dried over $MgSO_4$ and the solvent was removed. Flash chromatography on silica (24:1 CH_2Cl_2/CH_3OH) yielded **6** as a brown oil (2.74 g, 69.1 %). TLC R_f=0.67 (silica, 93:7:1 CH_2Cl_2/CH_3OH/NH_4OH); ^1H NMR (400 MHz, $CDCl_3$): δ = 8.46 (d, J=4.4 Hz, 2H, ArH), 7.47 (dt, J=7.7, 1.5 Hz, 2H, ArH), 7.22 (d, J=7.7 Hz, 2H, ArH), 7.03 (dd, J=5.1, 6.7 Hz, 2H, ArH), 6.88 (s, 1H, NH), 6.66 (dd, J=9.3, 5.1 Hz, 2H, ArH), 4.58 (s, 1H, CH), 3.83 (d, J=14.9 Hz, 2H, CH_2), 3.73 (d, J=14.9 Hz, 2H, CH_2), 3.79 (s, 3H, CH_3), 3.75 (s, 3H, CH_3), 2.84–2.75 (m, 2H, CH_2), 1.42 ppm (s, 9H, CH_3); ^{13}C NMR (100 MHz, $CDCl_3$): δ = 159.4, 156.2, 149.1, 149.0, 148.1, 136.5, 135.1, 123.1, 122.2, 118.5, 111.3, 109.8, 78.8, 60.5, 56.0, 55.8, 53.8, 28.6 ppm; IR (thin film): $\tilde{\nu}$ = 3357.2, 2972.9, 2931.7, 2833.9, 1703.3, 1590.9, 1513.3, 1464.3, 1364.2, 1252.7, 1163.8, 1144.5, 1025.6, 859.6, 760.4 cm^{-1}; HRMS (ESI+): m/z: calcd for: 478.2580; found: 478.2573 [M+H^+].

1-(3,4-Dimethoxyphenyl)-*N*′,*N*′-bispyridin-2-ylmethyl-ethane-1,2-diamine (7): Trifluoroacetic acid (CF_3CO_2H, 8 mL) was added to a solution of **6** (2.00 g, 7.18 mmol) in CH_2Cl_2 (40 mL) and stirred at 23 °C for 24 h. After removing the solvent, saturated aqueous K_2CO_3 (30 mL) was added to the reaction mixture and the product was extracted into CH_2Cl_2 (3× 60 mL). The combined organic extracts were dried over $MgSO_4$ and the solvent was removed to yield **7** as a brown oil (2.18 g, 80.1 %). TLC R_f= 0.36 (silica, 93:7:1 CH_2Cl_2/CH_3OH/NH_4OH); ^{1}H NMR (400 MHz, $CDCl_3$): δ = 9.42 (s, 2H, NH_2), 8.46 (d, J=4.0 Hz, 2H, ArH), 7.64 (t, J= 7.4 Hz, 2H, ArH), 7.27 (d, J=7.4 Hz, 2H, ArH), 7.19 (t, J=6.0 Hz, 2H, ArH), 7.05 (s, 1H, ArH), 6.89 (d, J=7.9 Hz, 1H, ArH), 6.70 (d, J= 8.3 Hz, 1H, ArH), 4.33 (d, J=8.8 Hz, 1H, CH), 4.07 (s, 4H, CH_2), 3.75 (s, 3H, CH_3), 3.69 (s, 3H, CH_3), 3.46 (d, J=12.4 Hz, 1H, CH_2), 3.12 ppm (d, J=13.1 Hz, 1H, CH_2); ^{13}C NMR (100 MHz, $CDCl_3$) 161.9, 161.5, 157.2, 149.5, 149.4, 147.0, 139.3, 127.7, 124.6, 123.4, 120.3, 118.4, 115.5, 111.4, 110.5, 60.2, 58.9, 56.0, 55.9, 54.3 ppm; IR (thin film): $\tilde{\nu}$ = 3057.0, 3009.0, 2939.3, 2841.0, 1671.1, 1595.7, 1519.7, 1466.3, 1426.1, 1265.0, 1197.5, 1175.1, 1125.3, 1023.9, 829.6, 798.1, 718.9 cm^{-1}; HRMS (ESI+): *m*/*z*: calcd for: 378.2056; found: 378.2050 [M+H$^+$].

1-(3,4-Dimethoxyphenyl)-*N*,*N*,*N*′,*N*′-tetrakispyridin-2-ylmethyl-ethane-1,2-diamine (8): Diamine **7** (2.00 g, 5.28 mmol) and 2-pyridinecarboxaldehyde (504 μL) were combined in EtOH (20 mL) and the solution was refluxed at 78 °C for 1 h. The solution was allowed to cool to 23 °C and $NaBH_4$ (399 mg, 10.6 mmol) was added. The reaction mixture was stirred at 23 °C for 24 h. After removing the solvent, saturated Na_2CO_3 (30 mL) was added and the product was extracted in to CH_2Cl_2 (3×60 mL). The combined organic extracts were dried over $MgSO_4$ and the solvent was removed. The crude product (2.24 g, 4.77 mmol) was dissolved in CH_2Cl_2 (40 mL) and treated with 2-pyridinecarboxaldehyde (455 μL, 4.77 mmol) and $NaBH(OAc)_3$ (2.02 g, 9.54 mmol). The reaction was stirred at 23 °C for 24 h. Saturated Na_2CO_3 (30 mL) was added and the product was extracted into CH_2Cl_2 (3×60 mL). The combined organic extracts were dried over $MgSO_4$ and the solvent was removed. Flash chromatography on silica (97:2:1→93:6:1 CH_2Cl_2/CH_3OH/NH_4OH) yielded **8** as a brown oil (1.52 g, 51.3 %). TLC R_f=0.38 (silica, 93:7:1 CH_2Cl_2/CH_3OH/NH_4OH); ^{1}H NMR (400 MHz, $CDCl_3$): δ = 8.45–8.39 (m, 4H, ArH), 7.56–7.39 (m, 6H, ArH), 7.09–7.01 (m, 6H, ArH), 6.77–6.65 (m, 3H, ArH), 3.97 (dd, J=8.7, 5.3 Hz, 1H, CH), 3.84 (s, 3H, CH_3), 3.81 (d, J= 3.6 Hz, 2H, CH_2), 3.76 (s, 2H, CH_2), 3.74 (s, 3H, CH_3), 3.66 (d, J= 4.6 Hz, 2H, CH_2), 3.53 (d, J=14.9 Hz, 2H, CH_2), 3.17 (dd, J=13.0, 5.2 Hz, 1H, CH_2), 3.07 ppm (dd, J=13.0, 9.0 Hz, 1H, CH_2); ^{13}C NMR (100 MHz, $CDCl_3$): δ = 160.5, 159.8, 159.6, 149.4, 149.2, 145.0, 148.9, 148.6, 148.3, 136.5, 136.4, 136.3, 131.0, 123.3, 123.2, 122.9, 122.5, 122.0, 121.9, 112.8, 111.1, 110.8, 110.6, 62.2, 61.1, 61.0, 57.2, 56.8, 56.1, 56.05, 56.0 ppm; IR (thin film): $\tilde{\nu}$ = 3060.6, 3006.3, 2932.9, 2832.8, 1589.2, 1560.7, 1513.3, 1471.4, 1432.4, 1364.0, 1258.1, 1234.3, 1143.9, 1026.7, 994.5, 809.3, 760.1, 730.6 cm^{-1}; HRMS (ESI+): *m*/*z*: calcd for: 560.2900; found: 560.2913 [M+H$^+$].

1-(4,5-Dimethoxy-2-nitrophenyl)-*N*,*N*,*N*′,*N*′-tetrakispyridin-2-ylmethyl-ethane-1,2-diamine (ZinCleav-2, 1): Trifluoromethanesulfonic acid (457 μL, 5.18 mmol) and fuming nitric acid (91.5 %, 118 μL, 2.59 mmol) were combined in CH_2Cl_2 (10 mL) and stirred vigorously at 23 °C for 30 min. The mixture was cooled to −42 °C using a CH_3CN/dry ice bath. A solution of the diamine **8** (207 mg, 0.37 mmol) dissolved in CH_2Cl_2 (2 mL) was added to the above mixture in one portion. The reaction mixture was stirred at −42 °C for 10 h. Saturated Na_2CO_3 (30 mL) was added and the product was extracted in to CH_2Cl_2 (3×20 mL). The combined organic extracts were dried over $MgSO_4$ and the solvent was removed. Flash chromatography on silica (91:8:1 CH_2Cl_2/CH_3OH/NH_4OH) yielded ZinCleav-2 as a yellow oil (32 mg, 14.4 %). TLC R_f=0.32 (silica, 24:1 CH_2Cl_2:CH_3OH); ^{1}H NMR (400 MHz, $CDCl_3$): δ = 8.50–8.345 (m, 4H, ArH), 7.52–7.49 (m, 5H, ArH), 7.41–7.79 (m, 2H, ArH), 7.09–7.01 (m, 7H, ArH), 4.79 (d, J=9.0 Hz, 1H, CH), 3.84 (s, 3H. CH_3), 3.81 (d, J= 3.6 Hz, 2H, CH_2), 3.77 (s, 2H, CH_2), 3.74 (s, 3H, CH_3), 3.67 (d, J= 14.1 Hz, 2H, CH_2), 3.53 (d, J=14.1 Hz, 2H, CH_2), 3.18 (dd, J=13.0, 6.0 Hz, 1H, CH_2), 3.06 ppm (dd, J=13.0, 9.0 Hz, 1H, CH_2); ^{13}C NMR (100 MHz, $CDCl_3$): δ = 162.5, 159.8, 159.6, 150.4, 152.4, 149.2, 145.8, 149.9, 148.6, 148.3, 136.5, 136.4, 131.0, 123.9, 122.9, 122.0, 121.9, 113.8, 112.1, 110.9, 110.7, 62.2, 61.1, 62.0, 58.2, 56.8, 56.1, 56.0 ppm; IR (thin film); $\tilde{\nu}$ = 3012.1, 2926.3, 2850.7, 1652.8, 1593.6, 1520.8, 1471.7, 1466.9, 1436.5, 1339.1, 1273.2, 1216.2, 1149.4, 1049.4, 795.1, 766.8 cm^{-1}; HRMS (ESI+): *m*/*z*: calcd for: 605.2751; found: 605.2763 [M+H$^+$].

General spectroscopic methods: All solutions were prepared with spectrophotometric grade solvents. HEPES (4-(2-hydroxyethyl)-1-piperazineethanesulfonic acid) and KCl (99.5 %) were purchased and used as received. Zn^{2+} stock solutions were prepared from 99.999 % pure $ZnCl_2$. All Zn^{2+} solutions were standardized by titrating with terpyridine and measurement of the absorption spectra. ZinCleav-2 was introduced to aqueous solution by addition of stock solution in DMSO (15.0 mM). Graphs were manipulated and equations calculated by using Kaleidagraph 4.0. The pH values of solutions were recorded with an Omega PHB 212 glass electrode that was calibrated prior to each use. Absorption spectra were recorded on a Cary 50 UV-visible spectrophotometer under the control of a Pentium IV-based PC running the manufacturer supplied software package. Spectra were routinely acquired at 25 °C, in 1 cm path length quartz cuvettes with a total volume of 3.0 mL. Fluorescence spectra were recorded on a Hitachi F-4500 spectrophotometer under the control of a Pentium-IV PC running the FL Solutions 2.0 software package. Excitation was provided by a 150 W Xe lamp (Ushio Inc.) operating at a current of 5 A. Spectra were routinely acquired at 25 °C, in 1 cm quartz cuvette with a total volume of 3.0 mL using, unless otherwise stated, 5 nm slit widths and a photomultiplier tube power of 700 V. Photolysis experiments were performed at 25 °C, in 1 cm path length quartz cuvettes illuminated by a 150 W Xe lamp of a Hitachi F-4500 spectrophotometer with emission wavelength set to 350 nm or a Rayonet RPR-100 Photochemical Reactor containing 12 bulbs (900 W), each emitting at 3500 Å. HPLC was performed on a Perkin–Elmer 250 binary pump equipped with a diode array detector under the control of a Pentium-III PC running the PeakSimple software package. An Ultra C18 column (250×4.6 mm) was used for the separation of photoproducts and the peaks were detected at 250 nm. A linear gradient from 50 % A in B to 100 % A was run at 0.8 mL min^{-1} for 30 min, where A is 2 % formic acid in water and B is MeOH.

Determination of Zn^{2+} binding constant

Calibration curve: A 10 μM solution of the fluorescent Zn^{2+} sensor **11** (25 mM HEPES, 100 mM $NaClO_4$, pH 7.4) was prepared. A 3.0 mL aliquot of this solution was placed in a quartz cuvette and fluorescence was measured. Ten 1.5 μL aliquots of a 1.0 mM $Zn(ClO_4)_2$ stock solution was added to the above solution and fluorescence was measured after each addition. Fluorescence was corrected for dilution, normalized and plotted against total Zn^{2+} concentration to generate a calibration curve.

Competitive titration with ZinCleav-2: To the above solution, 2.0 μL aliquots of a 15 mM ZinCleav-2 solution were added. Fluorescence of the solution was measured after each addition. No further decrease in fluorescence was observed after adding 30 equivalents (300 μM) of ZinCleav-2. Fluorescence was corrected for dilution and normalized. The above procedure was repeated three times. Under the experimental conditions 99.99 % of Zn^{2+} is bound to the sensor at the beginning of the titration. The binding equilibrium for this system may be expressed by Equation (1). The binding constant of the $[Zn(ZinCleav\text{-}2)]^{2+}$ complex ($K'_{ZinCleav\text{-}2}$) is obtained by solving Equation (2), where $K'_{ZnSensor\text{-}1}$=2.2 ×10^{15} M^{-1}.

$$ZinCleav + [Zn(ZnSensor)]^{2+} = [Zn(ZinCleav)]^{2+} + ZnSensor \quad (1)$$

$$\frac{[Zn(ZinCleav)]^{2+}[ZnSensor]}{[ZinCleav][Zn(ZnSensor)]^{2+}} = \frac{K'_{ZinCleav}}{K'_{ZnSensor}} \quad (2)$$

Equations (3)–(5) were used to calculate the individual components of Equation (2). [Zn(ZnSensor-1)] was determined from the calibration curve.

$$[ZnSensor] = [ZnSensor]_{total} - [Zn(ZnSensor)]^{2+} \quad (3)$$

$$[Zn(ZinCleav)]^{2+} = [Zn(ZnSensor)]^{2+}_{initial} - [Zn(ZnSensor)]^{2+} \quad (4)$$

$$[ZinCleav] = [ZinCleav]_{total} - [Zn(ZinCleav)] \quad (5)$$

Quantum efficiency of photolysis

Calibration curve: A 1.2 mM $[Zn(ZinCleav-2)]^{2+}$ stock solution was prepared. The stock solution was diluted to make 10, 30, 40, 50 and 60 μM $[Zn(ZinCleav-2)]^{2+}$ solutions. HPLC traces of each solution were recorded and the area under the curve was determined by integration.

Photolysis of $[Zn(ZinCleav-2)]^{2+}$: A 2.0 mL aliquot of a 60 μM solution was irradiated at 350 nm using a 150 W Xe lamp. HPLC traces of the above solution were recorded after irradiating for 60, 90 and 120 min. The area of the $[Zn(ZinCleav-2)]^{2+}$ peak was obtained by integration and the concentration of remaining $[Zn(ZinCleav-2)]^{2+}$ was determined using the calibration curve. The quantum efficiency of photolysis of ZinCleav-2 was obtained by solving equation 6 where N_A is the Avogadro's number.

$$\text{quantum efficiency} = \frac{\text{change in } [\text{ZinCleav} - 2]/\text{irradiation time}}{\text{intensity of the source}} N_A \qquad (6)$$

The intensity of the source was determined as described previously.[31] The quantum yield of photolysis of compounds **2**, **3** and **4** were determined by UV-visible spectroscopy as described previously.[31]

Cu/Zn exchange: A 2.0 mL aliquot of a 60 μM solution of ZinCleav-2 (40 mM HEPES, 100 mM KCl, pH 7.4) was placed in a quartz cuvette. A 24 μL aliquot of a $CuCl_2$ stock solution (50 mM) was added to give a final Cu^{2+} concentration of 600 μM, and the absorption spectrum was recorded. Another 2.0 mL aliquot of a 60 μM solution of ZinCleav-2 (40 mM HEPES, 100 mM KCl, pH 7.4) was placed in a quartz cuvette and a 12 μL aliquot of a $ZnCl_2$ stock solution (10 mM) was added to give final Zn^{2+} concentration of 60 μM. A 24 μL aliquot of a $CuCl_2$ stock solution (50 mM) was added to give a final Cu^{2+} concentration of 600 μM and the absorption spectrum was recorded. Absorption spectra were recorded at 5 min intervals for 30 min.

Ca/Zn exchange: A 2.0 mL aliquot of a 60 μM solution of ZinCleav-2 (40 mM HEPES, 100 mM KCl, pH 7.4) was placed in a quartz cuvette. A 24 μL aliquot of a $CaCl_2$ stock solution (0.50 M) was added to give a final Ca^{2+} concentration of 6.0 mM, and the absorption spectrum was recorded. A 12 μL aliquot of a $ZnCl_2$ stock solution (10 mM) was added to give final Zn^{2+} concentration of 60 μM and the absorption spectrum was recorded.

Release of caged Zn^{2+}: A 2.0 mL aliquot of a 5.0 μM ZinPyr-1 solution (40 mM HEPES, 100 mM KCl, pH 7.4) was placed in a quartz cuvette and the fluorescence spectrum was recorded. A 66 μL aliquot of a $ZnCl_2$ stock solution (9.02 mM) was added to give a final concentration of 30 μM and the fluorescence spectrum was recorded. A 40 μL aliquot of the ZinCleav-2 stock solution (2.0 mM) was added to give a final concentration of 40 μM and the fluorescence spectrum was recorded. The cuvette was irradiated in a Rayonet RPR-100 photoreactor with 350 nm wavelength radiation and the fluorescence spectra were recorded at 1 min intervals.

Acknowledgements

This work was supported by the University of Connecticut, the University of Connecticut Research Foundation grant PD09-0154 and by NSF grant CHE-0955361.

[1] J. Hébert, D. Gravel, *Can. J. Chem.* **1974**, *52*, 187–189.
[2] A. J. Kirby, G. A. Varvoglis, *Chem. Commun.* **1967**, 406.
[3] A. Patchornik, B. Amit, R. B. Woodward, *J. Am. Chem. Soc.* **1970**, *92*, 6333–6335.
[4] B. Amit, U. Zehavi, A. Patchornik, *J. Org. Chem.* **1974**, *39*, 192–196.
[5] J. Engels, E. J. Schlaeger, *J. Med. Chem.* **1977**, *20*, 907–911.
[6] U. Zehavi, B. Amit, A. Patchornik, *J. Org. Chem.* **1972**, *37*, 2281–2285.
[7] J. H. Kaplan, B. Forbush III, J. F. Hoffman, *Biochemistry* **1978**, *17*, 1929–1935.
[8] J. W. Walker, J. A. McCray, G. P. Hess, *Biochemistry* **1986**, *25*, 1799–1805.
[9] T. Milburn, N. Matsubara, A. P. Billington, J. B. Udgaonkar, J. W. Walker, B. K. Carpenter, W. W. Webb, J. Marque, W. Denk, J. A. McCray, G. P. Hess, *Biochemistry* **1989**, *28*, 49–55.
[10] R. Wieboldt, K. R. Gee, L. Niu, D. Ramesh, B. K. Carpenter, G. P. Hess, *Proc. Natl. Acad. Sci. USA* **1994**, *91*, 8752–8756.
[11] J. W. Walker, A. V. Somlyo, Y. E. Goldman, A. P. Somlyo, D. R. Trentham, *Nature* **1987**, *327*, 249–252.
[12] J. W. Walker, J. Feeney, D. R. Trentham, *Biochemistry* **1989**, *28*, 3272–3280.
[13] H. Ando, T. Furuta, R. Y. Tsien, H. Okamoto, *Nat. Genet.* **2001**, *28*, 317–325.
[14] W. T. Monroe, M. M. McQuain, M. S. Chang, J. S. Alexander, F. R. Haselton, *J. Biol. Chem.* **1999**, *274*, 20895–20900.
[15] J. W. Walker, S. H. Gilbert, R. M. Drummond, M. Yamada, R. Sreekumar, R. E. Carraway, M. Ikebe, F. S. Fay, *Proc. Natl. Acad. Sci. USA* **1998**, *95*, 1568–1573.
[16] D. M. Rothman, E. J. Petersson, M. E. Vazquez, G. S. Brandt, D. A. Dougherty, B. Imperiali, *J. Am. Chem. Soc.* **2005**, *127*, 846–847.
[17] G. Marriott, *Biochemistry* **1994**, *33*, 9092–9097.
[18] D. Mendel, J. A. Ellman, P. G. Schultz, *J. Am. Chem. Soc.* **1991**, *113*, 2758–2760.
[19] M. Ghosh, X. Song, G. Mouneimne, M. Sidani, D. S. Lawrence, J. S. Condeelis, *Science* **2004**, *304*, 743–746.
[20] N. Gagey, P. Neveu, L. Jullien, *Angew. Chem.* **2007**, *119*, 2519–2521; *Angew. Chem. Int. Ed.* **2007**, *46*, 2467–2469.
[21] M. J. Davis, C. H. Kragor, K. G. Reddie, H. C. Wilson, Y. Zhu, T. M. Dore, *J. Org. Chem.* **2009**, *74*, 1721–1729.
[22] R. Y. Tsien, R. S. Zucker, *Biophys. J.* **1986**, *50*, 843–853.
[23] S. R. Adams, J. P. Y. Kao, G. Grynkiewicz, A. Minta, R. Y. Tsien, *J. Am. Chem. Soc.* **1988**, *110*, 3212–3220.
[24] D. P. Kennedy, C. Gwizdala, S. C. Burdette, *Org. Lett.* **2009**, *11*, 2587–2590.
[25] D. P. Kennedy, C. D. Incarvito, S. C. Burdette, *Inorg. Chem.* **2010**, *49*, 916–923.
[26] C. Gwizdala, D. P. Kennedy, S. C. Burdette, *Chem. Commun.* **2009**, 6967–6969.
[27] G. C. R. Ellis-Davies, J. H. Kaplan, *Proc. Natl. Acad. Sci. USA* **1994**, *91*, 187–191.
[28] G. C. R. Ellis-Davies, J. H. Kaplan, *J. Org. Chem.* **1988**, *53*, 1966–1969.
[29] G. C. R. Ellis-Davies, *Cell Calcium* **2006**, *39*, 471–473.
[30] K. L. Ciesienski, K. L. Haas, M. G. Dickens, Y. T. Tesema, K. J. Franz, *J. Am. Chem. Soc.* **2008**, *130*, 12246–12247.
[31] H. M. D. Bandara, D. P. Kennedy, E. Akin, C. D. Incarvito, S. C. Burdette, *Inorg. Chem.* **2009**, *48*, 8445–8455.
[32] C. Jacob, W. Maret, B. L. Vallee, *Proc. Natl. Acad. Sci. USA* **1998**, *95*, 3489–3494.
[33] C. E. Outten, T. Y. O'Halloran, *Science* **2001**, *292*, 2488–2492.
[34] M. S. Nasir, C. J. Fahrni, D. A. Suhy, K. J. Kolodsick, C. P. Singer, T. V. O'Halloran, *J. Biol. Inorg. Chem.* **1999**, *4*, 775–783.
[35] S. C. Paski, Z. Xu, *J. Nutr. Biochem.* **2001**, *12*, 655–661.
[36] M. St Croix Claudette, K. J. Wasserloos, K. E. Dineley, I. J. Reynolds, E. S. Levitan, B. R. Pitt, *Am. J. Physiol.* **2002**, *282*, L185 L192.
[37] J. Cao, J. A. Bobo, J. P. Liuzzi, R. J. Cousins, *J. Leukocyte Biol.* **2001**, *70*, 559–566.
[38] Y. Mikata, M. Wakamatsu, A. Kawamura, N. Yamanaka, S. Yano, A. Odani, K. Morihiro, S. Tamotsu, *Inorg. Chem.* **2006**, *45*, 9262–9268.
[39] Y. Mikata, M. Wakamatsu, S. Yano, *Dalton Trans.* **2005**, 545–550.
[40] Y. Mikata, A. Yamanaka, A. Yamashita, S. Yano, *Inorg. Chem.* **2008**, *47*, 7295–7301.
[41] K. Hanaoka, Y. Muramatsu, Y. Urano, T. Terai, T. Nagano, *Chem. Eur. J.* **2010**, *16*, 568–572.
[42] J.-M. Lee, Y.-J. Kim, H. Ra, S.-J. Kang, S. Han, J.-Y. Koh, Y.-H. Kim, *FEBS Lett.* **2008**, *582*, 1871–1876.
[43] H.-H. Wang, Q. Gan, X.-J. Wang, L. Xue, S.-H. Liu, H. Jiang, *Org. Lett.* **2007**, *9*, 4995–4998.

[44] D. W. Gruenwedel, *Inorg. Chem.* **1968**, *7*, 495–501.
[45] J. H. Kaplan, G. C. R. Ellis-Davies, *Proc. Natl. Acad. Sci. USA* **1988**, *85*, 6571–6575.
[46] S. C. Burdette, G. K. Walkup, B. Spingler, R. Y. Tsien, S. J. Lippard, *J. Am. Chem. Soc.* **2001**, *123*, 7831–7841.
[47] B. A. Wong, S. Friedle, S. J. Lippard, *J. Am. Chem. Soc.* **2009**, *131*, 7142–7152.
[48] J. E. T. Corrie, A. Barth, V. R. N. Munasinghe, D. R. Trentham, M. C. Hutter, *J. Am. Chem. Soc.* **2003**, *125*, 8546–8554.
[49] M. Gaplovsky, Y. V. Il′ichev, Y. Kamdzhilov, S. V. Kombarova, M. Mac, M. A. Schworer, J. Wirz, *Photochem. Photobiol. Sci.* **2005**, *4*, 33–42.
[50] B. E. Cohen, B. L. Stoddard, D. E. Koshland, *Biochemistry* **1997**, *36*, 9035–9044.
[51] R. A. Bozym, R. B. Thompson, A. K. Stoddard, C. A. Fierke, *ACS Chem. Biol.* **2006**, *1*, 103–111.
[52] S. Overbeck, P. Uciechowski, M. L. Ackland, D. Ford, L. Rink, *J. Leukocyte Biol.* **2007**, *83*, 368–380.
[53] A. Krezel, W. Maret, *J. Biol. Inorg. Chem.* **2006**, *11*, 1049–1062.
[54] T. J. B. Simons, *J. Membr. Biol.* **1991**, *123*, 63–71.
[55] L. A. Finney, T. V. O'Halloran, *Science* **2003**, *300*, 931–936.
[56] L. Alderighi, P. Gans, A. Ienco, D. Peters, A. Sabatini, A. Vacca, *Coord. Chem. Rev.* **1999**, *184*, 311–318.
[57] G. C. R. Ellis-Davies, R. J. Barsotti, *Cell Calcium* **2006**, *39*, 75–83.

Received: July 13, 2010
Revised: October 26, 2010
Published online: March 1, 2011

